ORGANOMETALLICS
Article
Cite This: Organometallics XXXX, XXX, XXX−XXX
pubs.acs.org/Organometallics

Thermally Robust Heterobimetallic Palladium−Alkali Catalysts for Ethylene and Alkyl Acrylate Copolymerization

Zhongzheng Cai and Loi H. Do*

Department of Chemistry, University of Houston, 4800 Calhoun Road, Houston, Texas 77004, United States

Supporting Information

ABSTRACT: We report on the synthesis and characterization of a new family of palladium−alkali olefin polymerization catalysts using site-differentiated dinucleating platforms. Metal binding studies indicate that our palladium phosphine phosphonate polyethylene glycol (PEG) complexes form 1:1 adducts with alkali cations in solution, with relative affinities in the order $Na^+ \approx K^+ > Li^+$. We observed that these palladium−alkali complexes are more active for ethylene homopolymerization and ethylene/alkyl acrylate copolymerization in comparison to their monopalladium counterparts, although their effect on polymer branching and molecular weight is relatively modest. In some cases, the addition of external sodium salts to conventional palladium complexes (i.e., those that do not have pendant PEG chains) also led to remarkable catalyst enhancements, presumably also due to the formation of palladium−sodium species. The unique features of our heterobimetallic systems are that they display long catalyst lifetimes at 100 °C and can even operate at temperatures as high as 140 °C. Although we have shown that secondary cations clearly increase the electrophilicity of the metal catalyst, their precise role in these polymerization reactions is still under investigation.

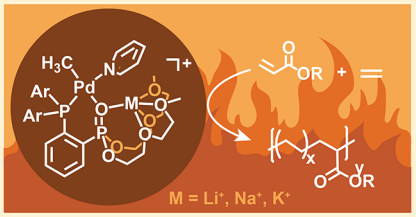

INTRODUCTION

Greater than 70% of the world's ethylene-based polymers is manufactured using transition-metal-catalyzed processes.[1] Because the intrinsic properties of polyolefins are determined by how their building blocks are assembled,[2] having a broad assortment of metal catalysts to synthesize polyolefins is required to meet the diverse needs of the global market. To be industrially useful, metal catalysts must also be highly active, tolerant of trace impurities, and compatible at high reactor temperatures (e.g., >80 °C).[3,4]

The discovery that cationic late-transition-metal diimine complexes are capable of copolymerizing ethylene with methyl acrylate[5] inspired many researchers to search for new families of polar group compatible molecular catalysts (Chart 1).[6−13] For example, the development of neutral palladium phosphine sulfonate complexes by Drent et al.[14] has enabled the copolymerization of ethylene with difficult to incorporate polar monomers such as vinyl acetate,[15] vinyl halide,[16,17] acrylonitrile,[18] and acrylamide.[19] Most recently, the research groups of Nozaki[20,21] and Jordan[22,23] disclosed that cationic palladium compounds ligated by P,O-ligands also gave active copolymerization catalysts.[24−26] A major drawback in many of these metal-based systems, however, is that the presence of polar monomers causes a significant decrease in catalytic activity in comparison to that in the presence of just ethylene.[9] Furthermore, the molecular weights of the copolymers also tend to be low ($M_n < 10^5$). In addition to other economic and environmental considerations (e.g., cost, time, waste, etc.), these shortcomings have thus prevented late transition metal complexes from being viable catalysts for commercial polyolefin synthesis.

Chart 1. Representative Examples of Late Transition Metal Catalysts for Olefin Homo- and Copolymerization

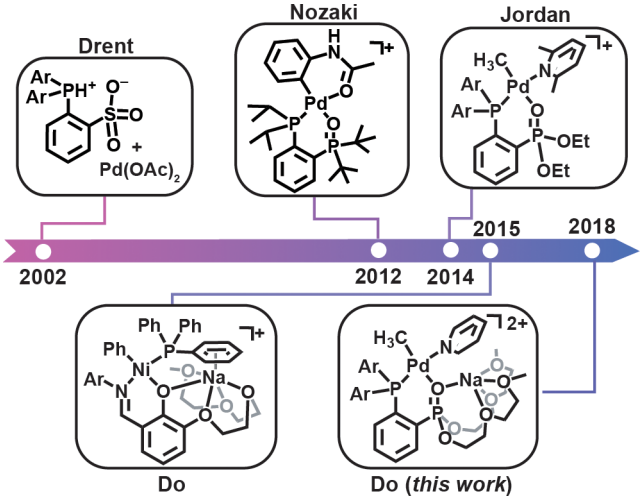

Our laboratory has been exploring new strategies to overcome the deficiencies of conventional olefin polymerization catalysts. We were inspired by several elegant examples in which Lewis acids were used successfully to promote diverse molecular transformations,[27] including carbon dioxide hydrogenation,[28,29] carbon monoxide insertion,[30,31] dihydrogen activation,[32,33] dioxygen activation,[34,35] and C−H bond oxidation.[36] In previous studies, we discovered that the incorporation of pendant Lewis acids into nickel phenox-

Received: August 4, 2018

DOI: 10.1021/acs.organomet.8b00561
Organometallics XXXX, XXX, XXX−XXX

yimine[37] polyethylene glycol (PEG) complexes led to a dramatic enhancement in their catalyst activity and changes to the microstructures of their polymer products.[38−40] An intriguing question that arose from this work was whether the performance-boosting effects of secondary cations is a general catalyst design feature that could be exploited in other molecular polymerization systems.[41] The underlying hypothesis in these studies is that catalysts bearing two functionally distinct metal centers (i.e., heterobimetallics) could work synergistically during polymerization to access reactivity patterns that could not be achieved using either monometallic or homobimetallic catalysts.[42−44] Specifically, secondary Lewis acids could modulate the electrophilicity of the active catalyst or assist in discrete steps during polymerization, such as monomer binding or chain propagation. Although we[38,39] and others[45] have shown that outer-sphere interactions with Lewis acidic metal cations could facilitate ethylene homopolymerization, their applications in ethylene and polar vinyl olefin copolymerization have not been explored extensively.[46]

Herein, we demonstrate that the pairing of alkali ions with palladium phosphine phosphonate ester complexes[22] imparts greater reactivity and thermal stability to the parent catalysts in both ethylene homo- and copolymerization. We show that the key to success is the installation of two PEG chains to the ligand's phosphonate group, which provides a well-defined binding site for alkali ions to yield discrete heterobimetallic species even in the presence of excess polar monomers.

RESULTS AND DISCUSSION

Synthesis of P,O-Ligands and Their Palladium Complexes. Our palladium phosphine phosphonate ester complexes were readily obtained through the synthetic sequence shown in Scheme 1. Lithiation of (2-bromophenyl)-diarylphosphine, followed by reaction with methyldiglycol chlorophosphate (**2**), provided ligands **3a** (Ar = phenyl) and **3b** (Ar = 2-methoxyphenyl) in moderate yields. Metalation of these ligands by treatment with Pd(COD)(Me)(Cl) (COD = 1,5-cyclooctadiene) gave complexes **4a** and **4b**, respectively. Chloride abstraction from **4a**/**4b** using $AgSbF_6$ and reaction with pyridine furnished complexes **5a**/**5b**. Single crystals of compounds **4b** and **5b** were analyzed by X-ray crystallography (Figure 1A and Figure S60, respectively). In both structures,

Scheme 1. Synthesis of Ligands 3 and Palladium Complexes 4 and 5

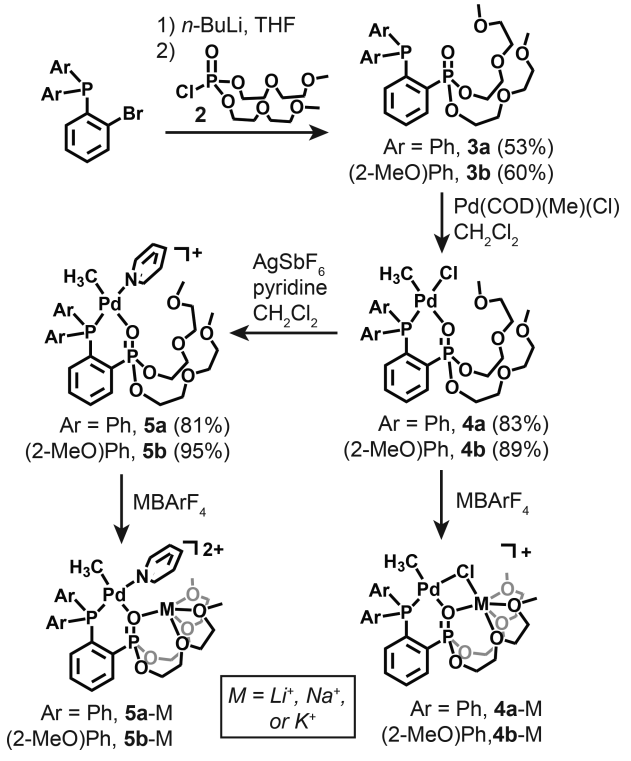

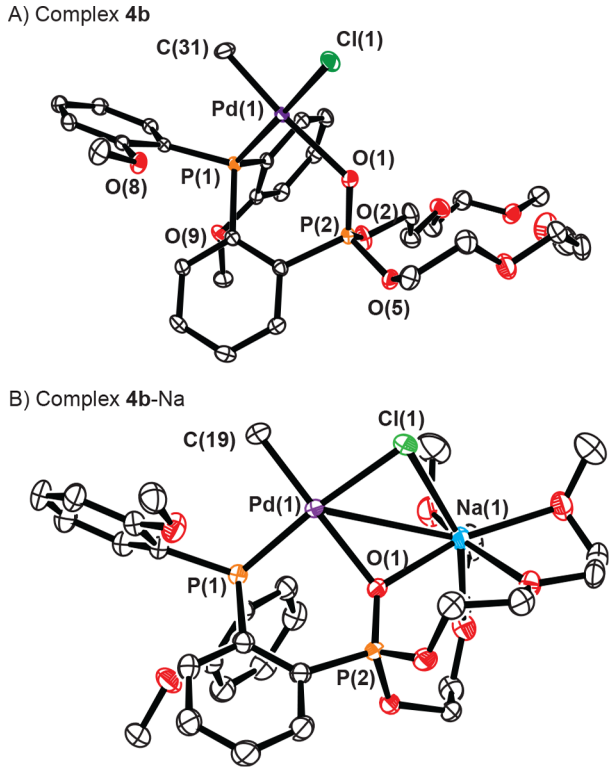

Figure 1. X-ray structures of the monopalladium **4b** (A) and heterobimetallic **4b**-Na (B) (ORTEP view, displacement ellipsoids drawn at 50% probability). Hydrogen atoms and borate anions are omitted for clarity.

the palladium center is square planar and the methyl group is trans to the phosphonate moiety. The bond metrics at the palladium core in **5b** are similar to those in the analogous diethylphosphonate variant reported by Jordan and co-workers.[22]

Secondary Alkali Ion Complexation. To investigate the interactions of our PEGylated palladium compounds with alkali ions, solution studies were carried out in chloroform. Using the method of continuous variation,[47,48] the NMR spectra of **4a** in the presence of various amounts of $MBAr^F_4$ salts ($M = Li^+$, Na^+, K^+; BAr^F_4 = tetrakis(3,5-trifluoromethylphenyl)borate) were recorded (Tables S1−S3). We observed that the H_{a1} and H_{a2} methylene hydrogen atoms in the PEG chains of **4a** (~4.1 ppm) showed greater chemical shift separations when larger amounts of M^+ were present (Figure 2 and Figures S1−S3).[49] This change in $\Delta\delta$ most likely reflects the different local environments of H_{a1} vs H_{a2} in the more rigid heterobimetallic structures in comparison to those in their monopalladium counterparts. The changes in the chemical shifts of H_{a1} were used to construct Job plots (Figure 3; X_{Pd} is defined as [**4a**]/([**4a**] + [M^+]). The peak

DOI: 10.1021/acs.organomet.8b00561
Organometallics XXXX, XXX, XXX−XXX

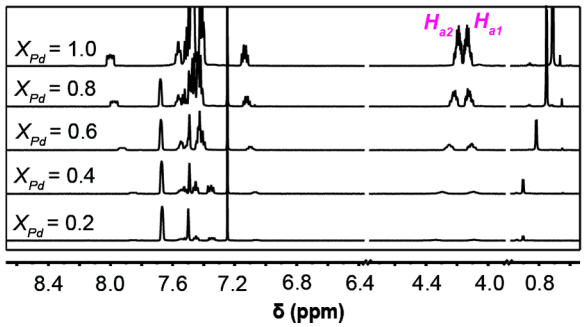

Figure 2. ^{1}H NMR spectra ($CDCl_3$, 600 MHz) of complex **4a** and $LiBAr^F_4$ mixed in different ratios. The mole fraction X_{Pd} is defined as [**4a**]/([**4a**] + [Li^+]). The peaks labeled as H_{a1} and H_{a2} are assigned to the methylene hydrogen atoms attached to carbon 1 of the PEG chains in **4a**.

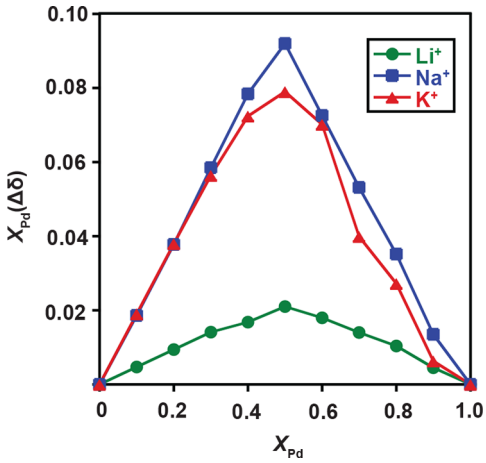

Figure 3. Job plots for complex **4a** with $MBAr^F_4$ (M = Li^+ (green circles), Na^+ (blue squares), K^+ (red triangles)) in $CDCl_3$. The total concentration of **4a**/$MBAr^F_4$ is 6 mM for all data points.

maxima of the Job plots for **4a**/M^+ all occur at X_{Pd} = 0.5, which indicates that a 1:1 stoichiometry is optimal between complex **4a** and alkali ions. The slopes of the three plots suggest that the alkali ion affinity of **4a** follows the order $Na^+ \approx K^+ > Li^+$. The dinuclear structure of the palladium−sodium complex **4b**-Na was confirmed by X-ray crystallographic analysis (Figure 1B). The structure revealed that the palladium center in **4b**-Na has the expected square-planar geometry, with slightly modified bond distances in comparison to those in **4b** (Pd−O and Pd−Cl are longer, whereas Pd−P and Pd−C are shorter). The sodium ion is six-coordinate due to ligation by five oxygen donors and a bridging chloride. The Pd−Na bond distance is ∼3.45 Å.

For complex **5b**, which contains a pyridine donor instead of chloride as in **4b**, similar alkali ion binding behavior was observed (Figures S4 and S5). Complexation of Na^+ to **5b** led to a downfield shift of the phosphine oxide signal at 22 ppm to 23 ppm in the ^{31}P NMR spectrum, which we have attributed to the electron-withdrawing effects of sodium. Complex **6b** ,on the other hand (Scheme 2), showed more minor changes in its NMR spectra when sodium salt was added in comparison to **5b** (Figures S6 and S7). These data suggest that, although **6b** can form adducts with Na^+, it does so more weakly than **5b**, which is expected since it lacks metal chelating PEG chains. Although our metal binding studies were performed in

Scheme 2. Reaction of Complex 6b with $NaBAr^F_4$ to Give 6b-Na[a]

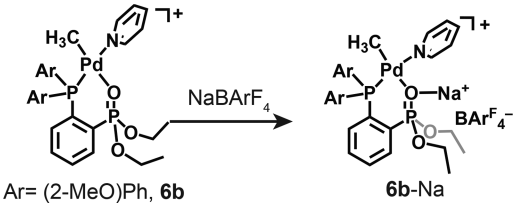

[a]The Na^+ cation is proposed to bind to the P═O donor of **6b**, but interactions with the other oxygen atoms of the phosphonate ester are also possible.

chloroform rather than in toluene, which is the solvent used in our polymerization studies below, we expect that the optimal 1:1 palladium−alkali binding stoichiometry should still be maintained in the latter.

To probe the electronic effect of M^+ on the palladium complexes, cyclic voltammetry measurements were conducted (Figure 4). Due to solubility reasons and the highly negative

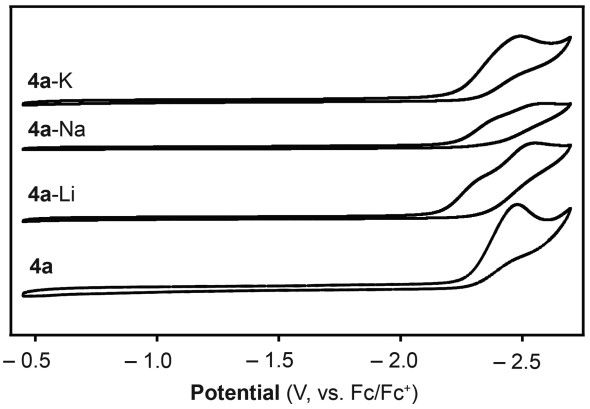

Figure 4. Cyclic voltammograms of complexes **4a**, **4a**-Li, **4a**-Na, and **4a**-K (1 mM, bottom to top) recorded in THF at 0.05 V/s in THF with 0.1 M NBu_4PF_6 supporting electrolyte. The data were acquired using a glassy-carbon working electrode, platinum counter electrode, and silver reference electrode. The reduction potentials measured are as follows: **4a**, −2.5 V; **4a**-Li, −2.2 and −2.5 V; **4a**-Na, −2.3 and −2.5 V; **4a**-K, −2.4 and −2.5 V (difficult to deconvolute due to peak broadness) (vs Fc/Fc^+). The peaks at −2.5 V are assigned to the presence of **4a** rather than from the heterobimetallic palladium−alkali species.

reduction potential of our compounds, THF was used as the electrochemical solvent. In the absence of M^+, **4a** displayed a cathodic peak at −2.5 V (vs ferrocene/ferrocenium), which we have tentatively assigned to reduction of the Pd(II) center. The cyclic voltammograms of **4a**-Li, **4a**-Na, and **4a**-K showed additional broad irreversible waves at approximately −2.2, −2.3, and −2.4 V, respectively,[50,51] and were ascribed to Pd-centered reduction processes in the heterobimetallic species. This trend is consistent with the electrophilicity of the alkali ions,[52] which would be expected to cause a decrease in the electron density at the palladium core through electronic induction.[53] We believe that,in THF, an appreciable amount of both monopalladium **4a** and heterobimetallic **4a**-M species are present in equilibrium due to the lower alkali ion binding affinity of **4a** in coordinating solvents in comparison to that in noncoordinating solvents (e.g., chloroform).

DOI: 10.1021/acs.organomet.8b00561
Organometallics XXXX, XXX, XXX−XXX

Table 1. Ethylene Homopolymerization Data for 5a,b and 6b[a]

entry	complex	salt	polymer yield (g)	activity (kg/(mol·h))	branches/1000 C[b]	$M_n(\times10^3)$[c]	M_w/M_n[c]
1	**5a**	none	trace	0			
2	**5a**	Na^+	trace	0			
3	**5b**	none	2.33	233	7	2.17	1.27
4	**5b**	Li^+	6.15	615	11	2.15	1.65
5	**5b**	Na^+	6.75	675	10	2.90	1.46
6	**5b**	K^+	4.67	467	8	2.90	1.50
7	**6b**	none	3.95	395	9	1.66	1.48
8	**6b**	Na^+	8.95	895	10	1.82	1.70

[a]Polymerization conditions: Pd catalyst (5 μmol), $MBAr^F_4$ (5 μmol, if any), ethylene (400 psi), 2 mL of DCM, 48 mL of toluene, 2 h at 80 °C. [b]The total number of branches per 1000 carbons was determined by ^1H NMR spectroscopy. [c]Determined by GPC in trichlorobenzene at 150 °C.

Ethylene Homopolymerization. Our palladium phosphine phosphonate PEG complexes were tested as catalysts for ethylene homopolymerization (Table 1). We found that, at 80 °C in toluene under 400 psi of ethylene, complex **5a** was completely inactive (entry 1) whereas complex **5b** displayed moderate activity (entry 3, activity = 233 kg/(mol·h)). The poor reactivity of **5a** is most likely due to the insufficient steric protection of the palladium center, which is typically required to help promote chain growth over chain termination. In comparison, the Jordan-type catalyst **6b** yielded polyethylene with an activity of 395 kg/(mol·h) under the same reaction conditions (entry 7).[22] In all cases, the polymers produced were relatively linear (10 branches or less per 1000 carbons) and their molecular weights are low ($M_n \approx (1.66–2.17) \times 10^3$), which is consistent with other reported Pd(P,O-ligand) systems.[21] The slower reaction rate of **5b** in comparison to that of **6b** suggests that the free PEG chains in the former might be self-inhibiting, perhaps by competing with ethylene for coordination to the palladium catalyst.

Next, we proceeded to evaluate the effects of alkali salts on the catalyst's reactivity toward ethylene (Table 1). Using the same polymerization conditions as above, we observed that the reaction of **5b** and $MBAr^F_4$ (1:1) with ethylene led to catalytic rate enhancements of about 2.6×, 2.9×, and 2.0× for Li^+ (entry 4), Na^+ (entry 5), and K^+ (entry 6), respectively, in comparison to **5b** alone. The polymer molecular weight and polydispersity remained relatively constant in both the presence and absence of alkali ions. The activity trend observed, $Na^+ > Li^+ > K^+$, was somewhat surprising because we noted previously that potassium ions had a more beneficial effect on nickel phenoxyimine-PEG catalysts than lithium ions.[38,39] In the current system, we hypothesize that a *combination* of at least two different factors account for the heterobimetallic effect—the electrophilicity (i.e., $Li^+ > Na^+ > K^+$)[52] and the association constant (i.e., $Na^+ \approx K^+ > Li^+$) of the secondary metals.

Interestingly, the reaction of **6b** and $NaBAr^F_4$ (1:1) with ethylene led to activity enhancements of about 2.3× in comparison to **6b** alone (Table 1, entry 7 vs 8). Because **6b** can associate weakly with Na^+, presumably via metal chelation by the phosphonate ester group (Figures S6 and S7), this result is consistent with our proposed heterobimetallic model. However, we have not discounted other possibilities, such as changes to the solvent medium due to the addition of salts. Since $NaBAr^F_4$ does not dissolve in neat toluene without either binding to the palladium catalyst first or mixing with surfactants, it is not likely to contribute to the ionic strength of the reaction solution. To support our claim that the introduction of PEG chains to the ligand platform is beneficial to catalyst stability, we observed that the palladium–sodium **6b**-Na complex is less active at high temperatures in comparison to PEG-ligated **5b**-Na compounds (vide infra).

Temperature Study. To determine the optimal reaction temperature, we screened several catalysts in ethylene polymerization from 80 to 140 °C in mesitylene/dichloromethane (24/1) for 1 h (Figure 5). For the compounds **5b**, **5b**-Na, **6b**, and **6b**-Na, reactions at 100 °C afforded the highest activity and their relative rates were generally observed in the order **5b**-Na > **6b**-Na > **6b** > **5b**. The only exception to this trend is that **6b-Na** is about 1.5× more active than **5b**-Na at 80 °C (Table S4, entry 5 vs 13). At elevated temperatures, however, the opposite was observed. For example, at 140 °C, **5b**-Na (1065 kg/(mol·h)) was about 1.8× faster than **6b**-Na (585 kg/(mol·h)). In this temperature regime, both palladium–sodium complexes were far more active than their corresponding parent **5b** and **6b** complexes (activity = 85 and 32 kg/(mol·h), respectively). Our temperature studies revealed two notable features of this catalyst system. First, for polymerizations conducted at 80 °C or below, the addition of stoichiometric amounts of alkali salts to standard palladium phosphine phosphonate ester complexes (e.g., those that are not functionalized with PEG chains) is sufficient to boost catalyst activity. Second, to maximize outer-sphere interactions at high temperatures, the catalyst supporting ligands should have suitably strong secondary metal chelators to prevent dissociation of the heterobimetallic structure.

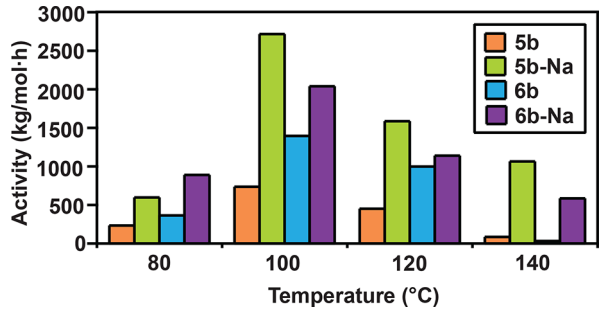

Figure 5. Comparison of the activities of catalysts **5b**, **5b**-Na, **6b**, and **6b**-Na in ethylene homopolymerization at various temperatures. See Table S4 for more details.

Time Study. To examine the catalyst lifetimes, we carried out time-dependent polymerizations for both complexes **5b**-Na and **6b** at 100 °C (Table S5). During the period from 15 to 60 min, both catalysts maintained their catalytic performance. However, **5b**-Na showed about an ~1.9× greater activity (average = 2605 kg/(mol·h)) than **6b** (average = 1343 kg/

DOI: 10.1021/acs.organomet.8b00561
Organometallics XXXX, XXX, XXX–XXX

Table 2. Ethylene and Alkyl Acrylate Copolymerization Data for 5b and 6b[a]

entry	comonomer (concn, M)	cat.	salt (equiv)	temp (°C)	polymer yield (g)	activity (kg/(mol·h))	branches/ 1000 C[b]	inc[c] (%)	M_n(×10^3)[d]	M_w/M_n[d]
1	MA (1.5)	**5b**	none	80	0.68	34	7	1.4	1.15	1.67
2	MA (1.5)	**5b**	Li^+ (1.0)	80	1.54	76	5	1.5	1.63	2.00
3	MA (1.5)	**5b**	Na^+ (1.0)	80	1.26	63	5	1.5	1.73	2.17
4	MA (1.5)	**5b**	Na^+ (5.0)	80	1.79	90	5	1.4	3.15	1.24
5	MA (1.5)	**5b**	K^+ (1.0)	80	1.22	61	5	1.3	1.99	2.00
6	MA (1.5)	**6b**	none	80	1.12	56	5	1.5	0.90	2.54
7	MA (1.5)	**6b**	Na^+ (1.0)	80	1.28	64	5	1.5	0.98	1.83
8[e]	BA (1.0)	**5b**	none	100	1.41	70	8	1.2	1.04	1.64
9[e]	BA (1.5)	**5b**	none	100	0.86	43	8	1.6	1.43	1.28
10[e]	BA (1.0)	**5b**	none	120	trace	0				
11[e]	BA (1.0)	**5b**	Na^+ (1.0)	100	1.67	84	6	1.2	2.30	1.47
12[e]	BA (1.5)	**5b**	Na^+ (1.0)	100	1.37	69	6	1.9	2.48	1.56
13[e]	BA (1.0)	**5b**	Na^+ (5.0)	100	1.44	72	6	1.7	2.14	1.41
14[e]	BA (1.0)	**5b**	Na^+ (1.0)	120	1.25	63	7	1.3	1.73	1.55
15[e]	BA (1.0)	**6b**	none	100	1.57	78	5	1.0	0.99	2.16
16[e]	BA (1.5)	**6b**	none	100	0.97	48	8	1.7	1.03	1.93
17[e]	BA (1.5)	**6b**	Na^+ (1.0)	100	1.13	56	8	1.6	1.14	2.07

[a]Polymerization conditions unless specified otherwise: Pd catalyst (10 μmol), $MBAr^F_4$ (10 μmol, if any), ethylene (400 psi), 50 mL total solution volume in toluene, 2 h. [b]The total number of branches per 1000 carbons was determined by ^{1}H NMR spectroscopy. [c]Determined by ^{1}H NMR spectroscopy. [d]Determined by GPC in trichlorobenzene at 150 °C. [e]These reactions were performed in mesitylene/dichloromethane (24/1) in a total volume of 50 mL.

(mol·h)). The thermal robustness of the **5b**-Na complex is exciting from an industrial standpoint because most large-scale commercial solution polymerizations are conducted at 140 °C or above.[3] In fact, homogeneous late-transition-metal catalysts that can operate within this temperature regime are relatively uncommon.[1,54−58]

Ethylene and Alkyl Acrylate Copolymerization. Finally, our palladium catalysts were tested in ethylene and methyl acrylate (MA) copolymerization (Table 2). The reaction of **5b** with ethylene/MA at 80 °C afforded linear poly(ethylene-*co*-methyl acrylate) containing ∼1.4 mol % of in-chain polar groups (entry 1). Under similar polymerization conditions, the **5b**-M complexes also furnished copolymers with low molecular weight and modest MA ratio. Consistent with our ethylene homopolymerization studies above, the heterobimetallic complexes were more active than their monopalladium counterparts. The highest activity was achieved using 5 equiv of $NaBAr^F_4$ relative to **5b**, which gave about a 2.6× improvement over that of the monopalladium complex itself (compare entry 1 vs entry 4). A slight increase in the copolymer M_n was also obtained in the presence of sodium ions (M_n = 3.15 × 10^3 for **5b**-Na vs 1.15 × 10^3 for **5b**). The polycrystalline copolymers displayed T_m values ranging from 102 to 113 °C (Table S7). Comparison of the polymerization results between **6b** (entry 6) vs **6b**-Na (entry 7) showed that the two catalysts behaved quite similarly, although **6b**-Na (64 kg/(mol·h)) is slightly more active than **6b** (56 kg/(mol·h)). Interestingly, the main differences between the Jordon-type catalyst **6b** and the heterobimetallic **5b**-M catalysts are that the latter consistently gave copolymers with somewhat higher activity and molecular weight. Although these heterobimetallic effects are relatively small, they do suggest that the addition of alkali salts is beneficial to the copolymerization reactions.

To determine whether methyl acrylate can displace the alkali ions from the heterobimetallic complexes, we measured the ^{1}H/^{31}P NMR spectra of **5b**-Na in the presence of MA (Figures S58 and S59). Interestingly, our data showed that the NMR spectra of **5b**-Na remained unchanged when up to 100 equiv of MA was added. An important point to keep in mind, however, is that under actual catalytic conditions the amount of MA present is greater than 7000× that of the palladium catalyst. Thus, is it entirely possible that in our polymerization reactions, the dissociation of Na^+ from **5b**-Na can occur much more readily.

To investigate the copolymerization behavior of our catalysts at high temperatures, we replaced MA with *tert*-butyl acrylate (BA) as the polar monomer (Table 2). In general, we observed that increasing the starting BA concentration enhanced the percentage of BA incorporation into the copolymer. Although the addition of sodium salts to **5b** led to modest increases in catalyst activity and molecular weight under certain conditions (e.g., entry 9 vs entry 12), its most pronounced effect was on the catalyst's thermal stability. For example, at 120 °C, the activity of **5b**-Na was 63 kg/(mol·h) (entry 14), whereas that of **5b** was nearly zero (entry 10). For benchmarking, the addition of Na^+ to **6b** led to a 1.2× improvement in reaction yield (entry 16 vs entry 17) at 100 °C. Importantly, all of the poly(ethylene-*co*-*tert*-butyl acrylate) obtained showed relatively narrow M_w/M_n values (1.28−2.23), which suggest that our heterobimetallic catalysts are single-site species.

CONCLUSION

In summary, we have provided a simple and versatile strategy to site selectively incorporate secondary metals into conventional palladium catalyst platforms. We have shown that the pairing of alkali ions with late-transition-metal complexes could lead to significant catalyst enhancements, including improvements in their reaction rates and thermal stability. A surprising result in this study was that the addition of external alkali salts to simple palladium phosphine diethylphosphonate complexes was sufficient to generate palladium−alkali species that are more active than their parent complexes. However, we found that the use of PEGylated palladium analogues could better

DOI: 10.1021/acs.organomet.8b00561
Organometallics XXXX, XXX, XXX−XXX

support secondary metals, which was most clearly demonstrated in high-temperature polymerization reactions.

This work raises several intriguing questions that still need to be addressed. First, it is unclear what the precise role of the secondary metals during polymerization is. As indicated by cyclic voltammetry measurements, the alkali ions increase the electrophilicity of the palladium complexes. At the same time, however, binding of the alkali metals also leads to bulking up of the catalyst structure. Thus, to what extent do steric vs electronic factors contribute to the heterobimetallic effect? The precise effects of steric or electronic variations on catalyst reactivity are sometimes difficult to rationalize, since other factors such as catalyst stability and solubility could also play a role.[59−61] Second, in our copolymerization studies, the heterobimetallic catalysts seemed to have little influence on the comonomer incorporation ratio in comparison to the monometallic catalyts. We have preliminary data suggesting that ethylene binding and insertion into palladium−alkyl acrylate intermediates is faster when secondary cations are present. However, how does this change affect the relative rates of other elementary steps in the polymerization process? Future studies will focus on investigating these and other questions, which we anticipate will lead to a better understanding of the use of outer-sphere Lewis acids in catalyst design. Ultimately, these studies will allow us to create novel catalyst constructs to access a wider range of ethylene-based polymers for both common and specialized applications.

EXPERIMENTAL SECTION

General Procedures. Commercial reagents were used as received. All air- and water-sensitive manipulations were performed using standard Schlenk techniques or under a nitrogen atmosphere using a glovebox. Anhydrous solvents were obtained from an Innovative Technology solvent drying system saturated with argon. High-purity polymer grade ethylene was obtained from Matheson TriGas without further purification. The compounds (2-bromophenyl)-diphenylphosphine[62] and Pd(COD)(Me)(Cl)[63] were prepared according to literature procedures.

NMR spectra were acquired using JEOL spectrometers (ECA-400, -500, and -600) and referenced using residual solvent peaks. All ^{13}C NMR spectra were proton decoupled. ^{31}P NMR spectra were referenced to phosphoric acid. For polymer characterization, we used the following techniques. ^{1}H NMR spectroscopy: each NMR sample contained ∼20 mg of polymer in 0.5 mL of 1,1,2,2-tetrachloroethane-d_2 (TCE-d_2) and was recorded on a 500 MHz spectrometer using standard acquisition parameters at 120 °C.[64] ^{13}C NMR spectroscopy: each NMR sample contained ∼50 mg of polymer and 50 mM (8.7 mg) chromium acetylacetonate $Cr(acac)_3$ in 0.5 mL of TCE-d_2 and was recorded at 120 °C (125 MHz). The samples were acquired using a 90° pulse of 11.7 μs, a relaxation delay of 4 s, an acquisition time of 0.81 s, and inverse gated decoupling. The samples were preheated for 30 min prior to data acquisition. The carbon spectra were assigned on the basis of the chemical shift values reported in the literature.[12] High-resolution mass spectra were obtained from the mass spectral facility at the University of Houston. Elemental analyses were performed by Atlantic Microlab.

Gel permeation chromatography (GPC) data were obtained using a Malvern high temperature GPC instrument equipped with refractive index, viscometer, and light scattering detectors at 150 °C with 1,2,4-trichlorobenzene (stabilized with 125 ppm BHT) as the mobile phase. A calibration curve was established using polystyrene standards in triple detection mode. All molecular weights reported are based on triple detection.

Synthesis. *Preparation of **4a**.* Inside the drybox, compound **3a** (117 mg, 0.21 mmol, 1.0 equiv) and Pd(COD)(Me)(Cl) (57 mg, 0.21 mmol, 1.0 equiv) were combined in a small vial and then dissolved in DCM (5 mL) at room temperature. The reaction mixture was stirred at room temperature for 1 h and then filtered through a pipet plug. The filtrate was dried under vacuum. Pentane was added to the residue and the mixture stirred until a white solid formed (125 mg, 0.18 mmol, 83%). ^{1}H NMR ($CDCl_3$, 600 MHz): δ (ppm) 7.98 (dd, J_{PH} = 5.2 Hz, J_{HH} = 2.0 Hz), 7.55−7.38 (m, 12H), 7.12 (m, 1H), 4.17−4.10 (m, 4H), 3.55−3.44 (m, 12H), 3.31 (s, 6H), 0.69 (d, J_{PH} = 2.4 Hz, 3H). ^{13}C NMR ($CDCl_3$, 100 MHz): δ (ppm) 136.62 (m), 134.83 (m), 134.45 (d, J_{PC} = 12.7 Hz), 133.16 (m), 132.79 (m), 131.21, 130.76 (d, J_{PC} = 13.2 Hz), 129.63, 129.13, 128.88 (d, J_{PC} = 10.7 Hz), 71.87, 70.35, 69.82 (d, J_{PC} = 6.8 Hz), 66.82 (d, J_{PC} = 5.8 Hz), 59.13, 0.93 (*note: the signals in the aromatic region could not be assigned due to overlapping peaks*). ^{31}P NMR ($CDCl_3$, 162 MHz): δ (ppm) 32.15 (d, J_{PP} = 13 Hz), 20.76 (d, J_{PP} = 13 Hz). Anal. Calcd for $C_{29}H_{39}ClO_7P_2Pd$: C, 49.52; H, 5.59. Found: C,49.34; H, 5.55.

*Preparation of **4b**.* Inside the drybox, compound **3b** (165 mg, 0.27 mmol, 1.0 equiv) and Pd(COD)(Me)(Cl) (72 mg, 0.27 mmol, 1.0 equiv) were combined in a small vial and then dissolved in DCM (5 mL) at room temperature. The reaction mixture was stirred at room temperature for 1 h and then filtered through a pipet plug. The filtrate was dried under vacuum and washed with Et_2O to form a white solid (185 mg, 0.24 mmol, 89%). ^{1}H NMR ($CDCl_3$, 600 MHz): δ (ppm) 7.88 (m, 1H), 7.51−7.46 (m, 3H), 7.41 (t, J_{HH} = 7.2 Hz, 1H), 7.34 (br s, 1H), 7.29−7.25 (m, 2H), 6.95 (t, J_{HH} = 7.2 Hz, 2H), 6.91 (dd, J_{HH} = 8.4 Hz, J_{PH} = 4.8 Hz, 2H), 4.22−4.07 (m, 4H), 3.64 (s, 6H), 3.61−3.46 (m, 12H), 3.34 (s, 6H), 0.57 (d, J_{PH} = 3 Hz, 3H). ^{13}C NMR ($CDCl_3$, 125 MHz): δ (ppm) 160.72 (d, J_{PC} = 3.8 Hz), 136.52, 136.50 (dd, J_{PC} = 34.9, 10.7 Hz), 134.50 (d, J_{PC} = 15.9 Hz), 134.10 (t, J_{PC} = 6.4 Hz), 133.30, 131.45 (dd, J_{PC} = 6.1, 2.5 Hz), 130.26 (dd, J_{PC} = 185.8, 17.1 Hz), 129.82 (d, J_{PC} = 13.5 Hz), 120.92 (d, J_{PC} = 9.8 Hz), 116.14 (d, J_{PC} = 51.4 Hz), 111.23 (d, J_{PC} = 5.0 Hz), 71.87, 70.35, 70.03 (d, J_{PC} = 7.4 Hz), 66.54 (d, J_{PC} = 6.1 Hz), 59.11, 55.47, −0.22. ^{31}P NMR ($CDCl_3$, 243 MHz): δ (ppm) 23.39 (d, J_{PP} = 8.3 Hz), 21.51 (d, J_{PP} = 8.2 Hz). Anal. Calcd for $C_{31}H_{43}ClO_9P_2Pd$: C, 48.77; H, 5.68. Found: C, 48.75; H, 5.85.

*Preparation of **5a**.* Inside the drybox, **4a** (76 mg, 0.11 mmol, 1.0 equiv) and $AgSbF_6$ (37 mg, 0.11 mmol, 1.0 equiv) were combined in a small vial. A solution of DCM (5 mL) and pyridine (0.1 mL) was added at room temperature, and the reaction mixture was stirred for 1 h. The mixture was then filtered through a pipet plug and the filtrate was dried under vacuum. A solution of Et_2O was added to wash the residue to give a sticky oil (86 mg, 0.09 mmol, 81%). Trace amounts of residual solvent could not be removed completely by vacuum drying. ^{1}H NMR ($CDCl_3$, 400 MHz): δ (ppm) 8.71 (d, J_{HH} = 4.8 Hz, 2H), 8.13 (m, 1H), 7.93 (m, 1H), 7.67−7.47 (m, 14H), 7.15 (m, 1H), 4.07 (m, 4H), 3.54−3.39 (m, 12H), 3.32 (s, 6H), 0.58 (d, J_{PH} = 3.2 Hz, 3H). ^{13}C NMR ($CDCl_3$, 100 MHz): δ (ppm) 150.11, 139.26, 135.44 (m), 134.99 (m), 134.35 (d, J_{PC} = 9.9 Hz), 133.41 (m), 131.97, 131.60, 131.49 (m), 129.39 (d, J_{PC} = 8.8 Hz), 128.29, 127.86, 125.86, 71.76, 70.25, 69.34 (d, J_{PC} = 5.9 Hz), 67.39 (d, J_{PC} = 5.8 Hz), 59.01, 3.95 (*note: the signals in the aromatic region could not be assigned due to overlapping peaks*). ^{31}P NMR ($CDCl_3$, 243 MHz): δ (ppm) 33.11 (d, J_{PP} = 19.4 Hz), 21.01 (d, J_{PP} = 19.4 Hz).

*Preparation of **5b**.* Inside the drybox, **4b** (155 mg, 0.20 mmol, 1.0 equiv) and $AgSbF_6$ (70 mg, 0.20 mmol, 1.0 equiv) were combined in a small vial. A solution of DCM (10 mL) and pyridine (0.1 mL) was added at room temperature, and the reaction mixture was stirred for 1 h. The mixture was then filtered through a pipet plug and the filtrate was dried under vacuum. A solution of Et_2O was added to wash the residue to give a sticky oil (201 mg, 0.19 mmol, 95%). Trace amounts of residual solvent could not be removed completely by vacuum drying. ^{1}H NMR ($CDCl_3$, 600 MHz): δ (ppm) 8.67 (d, J_{HH} = 3.6 Hz, 2H), 7.97 (m, 1H), 7.92 (t, J_{HH} = 7.2 Hz, 1H), 7.58−7.56 (m, 5H), 7.51 (t, 7.8 Hz, 1H), 7.43−7.31 (m, 3H), 7.05 (t, J_{HH} = 7.8 Hz, 2H), 6.99 (dd, J_{HH} = 8.4 Hz, J_{HH} = 4.8 Hz, 2H), 4.00−3.87 (m, 4H), 3.68 (s, 6H), 3.54−3.42 (m, 12H), 3.32 (s, 6H), 0.39 (d, J_{PH} = 3.6 Hz, 3H). ^{13}C NMR ($CDCl_3$, 100 MHz): δ (ppm) 160.70 (d, J_{PC} = 2.9 Hz), 150.15, 139.02, 136.80 (d, J_{PC} = 11.7 Hz), 135.03 (d, J_{PC} = 16.5 Hz), 134.62 (dd, J_{PC} = 26.2, 3.6 Hz), 134.36, 134.05 (t, J_{PC} = 8.3 Hz), 132.15 (d, J_{PC} = 16 Hz), 130.52 (d, J_{PC} = 14.5 Hz), 128.95 (dd, J_{PC} =

DOI: 10.1021/acs.organomet.8b00561
Organometallics XXXX, XXX, XXX−XXX

187.6, 17.6 Hz), 125.70, 121.27 (d, J_{PC} = 11.6 Hz), 114.49 (d, J_{PC} = 56 Hz), 111.73, 71.77, 70.28, 69.42 (d, J_{PC} = 5.8 Hz), 66.84 (d, J_{PC} = 6.8 Hz), 59.02, 55.56, 3.19. ^{31}P NMR ($CDCl_3$, 243 MHz): δ (ppm) 23.93 (d, J_{PP} = 14.3 Hz), 21.54 (d, J_{PP} = 14.3 Hz).

Preparation of ***6b****.* Inside the drybox, the palladium phosphine diethylphosphonate chloride complex[22] (115 mg, 0.19 mmol, 1.0 equiv) and $AgSbF_6$ (65 mg, 0.19 mmol, 1.0 equiv) were combined in a small vial. A solution of DCM (10 mL) and pyridine (0.1 mL) was added at room temperature, and the reaction mixture was stirred for 1 h. The mixture was then filtered through a pipet plug and the filtrate was dried under vacuum. A solution of Et_2O was added to wash the residue to give a white solid (149 mg, 0.17 mmol, 89%). ^{1}H NMR ($CDCl_3$, 600 MHz): δ (ppm) 8.66 (d, J_{HH} = 4.9 Hz, 2H), 7.93 (t, 7.8 Hz, 1H), 7.83 (m, 1H), 7.62−7.53 (m, 6H), 7.38−7.34 (m, 3H), 7.05 (t, J_{HH} = 7.5 Hz, 2H), 6.99 (dd, J_{HH} = 8.4 Hz, J_{HH} = 4.8 Hz, 2H), 3.87(m, 4H), 3.68 (s, 6H), 1.10 (t, J_{HH} = 7.0 Hz, 6H), 0.38 (d, J_{PH} = 3.0 Hz, 3H). ^{13}C NMR ($CDCl_3$, 100 MHz): δ (ppm) 160.66 (d, J_{PC} = 2.2 Hz), 150.11, 139.14, 136.81 (d, J_{PC} = 11.3 Hz), 135.24 (d, J_{PC} = 14.1 Hz), 134.80 (dd. J_{PC} = 46.7, 11.4 Hz) 134.36, 133.42 (dd, J_{PC} = 9.3, 8.2 Hz), 132.11 (d, J_{PC} = 7.0 Hz), 130.63 (d, J_{PC} = 12.2 Hz), 129.18 (dd, J_{PC} = 184.7, 17.5 Hz) 125.74, 121.24 (d, J_{PC} = 11.3 Hz), 114.49 (d, J_{PC} = 56 Hz), 111.73 (d, J_{PC} = 4.4 Hz), 64.44 (d, J_{PC} = 6.4 Hz), 55.58, 15.89 (d, J_{PC} = 6.5 Hz), 3.12. ^{31}P NMR ($CDCl_3$, 243 MHz): δ (ppm) 24.11 (d, J_{PP} = 14.1 Hz), 21.08 (d, J_{PP} = 14.1 Hz).

Metal Binding Studies. The method of continuous variation (Job plot analysis) was used to determine the binding stoichiometry of our palladium complexes with alkali ions.[48] To perform these experiments, stock solutions of **4a** (6 mM, 6 mL) and $MBAr^F_4$ (6 mM, 15 equiv of Et_2O to solubilize the salts, 6 mL, M = Li^+, Na^+, K^+) were prepared separately in $CDCl_3$. Various amounts of each stock solution were placed in an NMR tube so that a total volume of 1 mL was obtained. Ten different NMR samples were prepared, each containing a different **4a**:M ratio. The samples were recorded at room temperature by ^{1}H NMR spectroscopy. As shown in Figures S1−S3, the two hydrogen resonances centered at ∼4.1 ppm corresponding to the C1 methylene unit of the PEG chains in **4a** shift in the presence of alkali ions. The chemical shift separation between H_{a1} and H_{a2} increases as the Pd mole fraction decreases. The changes in the ^{1}H NMR signals of H_a as a function of the mole fraction of **4a** are provided in Tables S1−S3.

Ethylene Polymerization. Inside the drybox, the palladium complexes (5 μmol) and alkali salts (5 μmol) were dissolved in 10 mL of toluene/DCM (8/2) and stirred for 10 min. By visual inspection, the resulting palladium−alkali complexes appeared to be soluble in the reaction mixture. The mixture was sealed inside a vial using a rubber septum and brought outside of the drybox. Under an atmosphere of N_2, the catalyst solution was loaded into a syringe. To prepare the polymerization reactor, 40 mL of dry toluene was placed in an empty autoclave and preheated to the desired temperature. The autoclave was purged with ethylene (20 psi) for 1 min, and then the catalyst solution was injected into the autoclave via syringe. The reactor pressure was increased to 400 psi of ethylene, and the contents were stirred vigorously for 2 h. To stop the polymerization, the autoclave was vented and cooled in an ice bath. A solution of MeOH (100−200 mL) was added to precipitate the polymer. The polymer was collected by vacuum filtration, rinsed with MeOH, and dried under vacuum at 80 °C overnight. The reported yields are average values of triplicate runs and typically have less than 5% deviation by weight.

Ethylene and Alkyl Acrylate Copolymerization. Inside the drybox, the palladium complexes (10 μmol) and alkali salts (10 μmol) were dissolved in 2 mL of DCM and stirred for 10 min. The mixture was sealed inside a vial using a rubber septum and brought outside of the drybox. Under an atmosphere of N_2, the alkyl acrylate comonomer was added to the catalyst solution and the final mixture was loaded into a syringe. To prepare the polymerization reactor, 39−41 mL of dry toluene or mesitylene was placed in an empty autoclave and preheated to the desired temperature. The autoclave was purged with ethylene (20 psi) for 1 min, and then the catalyst solution was injected into the autoclave via syringe. The reactor pressure was increased to 400 psi of ethylene and the contents were stirred vigorously for 2 h. To stop the polymerization, the autoclave was vented and cooled in an ice bath. A solution of MeOH (100−200 mL) was added to precipitate the polymer. The polymer was collected by vacuum filtration, rinsed with MeOH, and dried under vacuum at 80 °C overnight. The reported yields are average values of triplicate runs and typically have less than 5% deviation by weight.

■ ASSOCIATED CONTENT

Supporting Information

The Supporting Information is available free of charge on the ACS Publications website at DOI: 10.1021/acs.organomet.8b00561.

Experimental procedures, characterization of compounds and polymers, NMR spectra, and crystallographic data (PDF)

Accession Codes

CCDC 1848561−1848563 contain the supplementary crystallographic data for this paper. These data can be obtained free of charge via www.ccdc.cam.ac.uk/data_request/cif, or by emailing data_request@ccdc.cam.ac.uk, or by contacting The Cambridge Crystallographic Data Centre, 12 Union Road, Cambridge CB2 1EZ, UK; fax: +44 1223 336033.

■ AUTHOR INFORMATION

Corresponding Author

*E-mail for L.H.D.: loido@uh.edu.

ORCID

Loi H. Do: 0000-0002-8859-141X

Notes

The authors declare no competing financial interest.

■ ACKNOWLEDGMENTS

We are grateful to the Welch Foundation (Grant No. E-1894), the ACS Petroleum Research Fund (Grant No. 54834-DNI3), and the National Science Foundation (Grant No. CHE-1750411) for their generous support of this research. We also thank Po-Ni Lai for help with cyclic voltammetry measurements and Prof. Tom Teets for use of a potentiostat.

■ REFERENCES

(1) Klosin, J.; Fontaine, P. P.; Figueroa, R. Development of Group IV Molecular Catalysts for High Temperature Ethylene-α-Olefin Copolymerization Reactions. *Acc. Chem. Res.* **2015**, *48*, 2004−2016.

(2) Chung, T. C. M. *Functionalization of Polyolefins*; Academic Press: San Diego, CA, 2002.

(3) Xie, T.; McAuley, K. B.; Hsu, J. C. C.; Bacon, D. W. Gas Phase Ethylene Polymerization: Production Processes, Polymer Properties, and Reactor Modeling. *Ind. Eng. Chem. Res.* **1994**, *33*, 449−479.

(4) Ali, E. M.; Abasaeed, A. E.; Al-Zahrani, S. M. Optimization and Control of Industrial Gas-Phase Ethylene Polymerization Reactors. *Ind. Eng. Chem. Res.* **1998**, *37*, 3414−3423.

(5) Johnson, L. K.; Mecking, S.; Brookhart, M. Copolymerization of Ethylene and Propylene with Functionalized Vinyl Monomers by Palladium(II) Catalysts. *J. Am. Chem. Soc.* **1996**, *118*, 267−268.

(6) Boffa, L. S.; Novak, B. M. Copolymerization of Polar Monomers with Olefins Using Transition-Metal Complexes. *Chem. Rev.* **2000**, *100*, 1479−1493.

(7) Ittel, S. D.; Johnson, L. K.; Brookhart, M. Late-Metal Catalysts for Ethylene Homo- and Copolymerization. *Chem. Rev.* **2000**, *100*, 1169−1203.

(8) Nakamura, A.; Anselment, T. M. J.; Claverie, J.; Goodall, B.; Jordan, R. F.; Mecking, S.; Rieger, B.; Sen, A.; van Leeuwen, P. W. N. M.; Nozaki, K. Ortho-Phosphinobenzenesulfonate: A Superb Ligand

DOI: 10.1021/acs.organomet.8b00561
Organometallics XXXX, XXX, XXX−XXX

for Palladium-Catalyzed Coordination-Insertion Copolymerization of Polar Vinyl Monomers. *Acc. Chem. Res.* **2013**, *46*, 1438−1449.
(9) Nakamura, A.; Ito, S.; Nozaki, K. Coordination-Insertion Copolymerization of Fundamental Polar Monomers. *Chem. Rev.* **2009**, *109*, 5215−5244.
(10) Chen, C. Designing Catalysts for Olefin Polymerization and Copolymerization: Beyond Electronic and Steric Tuning. *Nat. Rev. Chem.* **2018**, *2*, 6−14.
(11) Radlauer, M. R.; Buckley, A. K.; Henling, L. M.; Agapie, T. Bimetallic Coordination Insertion Polymerization of Unprotected Polar Monomers: Copolymerization of Amino Olefins and Ethylene by Dinickel Bisphenoxyiminato Catalysts. *J. Am. Chem. Soc.* **2013**, *135*, 3784−3787.
(12) Xin, B. S.; Sato, N.; Tanna, A.; Oishi, Y.; Konishi, Y.; Shimizu, F. Nickel Catalyzed Copolymerization of Ethylene and Alkyl Acrylates. *J. Am. Chem. Soc.* **2017**, *139*, 3611−3614.
(13) Zhang, Y.; Mu, H.; Pan, L.; Wang, X.; Li, Y. Robust Bulky [P,O] Neutral Nickel Catalysts for Copolymerization of Ethylene with Polar Vinyl Monomers. *ACS Catal.* **2018**, *8*, 5963−5976.
(14) Drent, E.; van Dijk, R.; van Ginkel, R.; van Oort, B.; Pugh, R. I. Palladium Catalysed Copolymerisation of Ethene with Alkylacrylates: Polar Comonomer Built into the Linear Polymer Chain. *Chem. Commun.* **2002**, 744−745.
(15) Ito, S.; Munakata, K.; Nakamura, A.; Nozaki, K. Copolymerization of Vinyl Acetate with Ethylene by Palladium/Alkylphosphine−Sulfonate Catalysts. *J. Am. Chem. Soc.* **2009**, *131*, 14606−14607.
(16) Wada, S.; Jordan, R. F. Olefin Insertion into a Pd−F Bond: Catalyst Reactivation Following β-F Elimination in Ethylene/Vinyl Fluoride Copolymerization. *Angew. Chem., Int. Ed.* **2017**, *56*, 1820−1824.
(17) Weng, W.; Shen, Z.; Jordan, R. F. Copolymerization of Ethylene and Vinyl Fluoride by (Phosphine-Sulfonate)Pd(Me)(py) Catalysts. *J. Am. Chem. Soc.* **2007**, *129*, 15450−15451.
(18) Kochi, T.; Noda, S.; Yoshimura, K.; Nozaki, K. Formation of Linear Copolymers of Ethylene and Acrylonitrile Catalyzed by Phosphine Sulfonate Palladium Complexes. *J. Am. Chem. Soc.* **2007**, *129*, 8948−8949.
(19) Friedberger, T.; Wucher, P.; Mecking, S. Mechanistic Insights into Polar Monomer Insertion Polymerization from Acrylamides. *J. Am. Chem. Soc.* **2012**, *134*, 1010−1018.
(20) Carrow, B. P.; Nozaki, K. Synthesis of Functional Polyolefins Using Cationic Bisphosphine Monoxide−Palladium Complexes. *J. Am. Chem. Soc.* **2012**, *134*, 8802−8805.
(21) Carrow, B. P.; Nozaki, K. Transition-Metal-Catalyzed Functional Polyolefin Synthesis: Effecting Control Through Chelating Ancillary Ligand Design and Mechanistic Insights. *Macromolecules* **2014**, *47*, 2541−2555.
(22) Contrella, N. D.; Sampson, J. R.; Jordan, R. F. Copolymerization of Ethylene and Methyl Acrylate by Cationic Palladium Catalysts That Contain Phosphine-Diethyl Phosphonate Ancillary Ligands. *Organometallics* **2014**, *33*, 3546−3555.
(23) Johnson, A. M.; Contrella, N. D.; Sampson, J. R.; Zheng, M.; Jordan, R. F. Allosteric Effects in Ethylene Polymerization Catalysis. Enhancement of Performance of Phosphine-Phosphinate and Phosphine-Phosphonate Palladium Alkyl Catalysts by Remote Binding of $B(C_6F_5)_3$. *Organometallics* **2017**, *36*, 4990−5002.
(24) Chen, M.; Chen, C. A Versatile Ligand Platform for Palladium- and Nickel-Catalyzed Ethylene Copolymerization with Polar Monomers. *Angew. Chem., Int. Ed.* **2018**, *57*, 3094−3098.
(25) Zhang, W.; Waddell, P. M.; Tiedemann, M. A.; Padilla, C. E.; Mei, J.; Chen, L.; Carrow, B. P. Electron-Rich Metal Cations Enable Synthesis of High Molecular Weight, Linear Functional Polyethylenes. *J. Am. Chem. Soc.* **2018**, *140*, 8841−8850.
(26) Mitsushige, Y.; Yasuda, H.; Carrow, B. P.; Ito, S.; Kobayashi, M.; Tayano, T.; Watanabe, Y.; Okuno, Y.; Hayashi, S.; Kuroda, J.; Okumura, Y.; Nozaki, K. Methylene-Bridged Bisphosphine Monoxide Ligands for Palladium-Catalyzed Copolymerization of Ethylene and Polar Monomers. *ACS Macro Lett.* **2018**, *7*, 305−311.
(27) Maity, A.; Teets, T. S. Main Group Lewis Acid-Mediated Transformations of Transition-Metal Hydride Complexes. *Chem. Rev.* **2016**, *116*, 8873−8911.
(28) Bernskoetter, W. H.; Hazari, N. Reversible Hydrogenation of Carbon Dioxide to Formic Acid and Methanol: Lewis Acid Enhancement of Base Metal Catalysts. *Acc. Chem. Res.* **2017**, *50*, 1049−1058.
(29) Chakraborty, S.; Zhang, J.; Krause, J. A.; Guan, H. An Efficient Nickel Catalyst for the Reduction of Carbon Dioxide with a Borane. *J. Am. Chem. Soc.* **2010**, *132*, 8872−8873.
(30) Hazari, A.; Labinger, J. A.; Bercaw, J. E. A Versatile Ligand Platform that Supports Lewis Acid Promoted Migratory Insertion. *Angew. Chem., Int. Ed.* **2012**, *51*, 8268−8271.
(31) Gregor, L. C.; Grajeda, J.; White, P. S.; Vetter, A. J.; Miller, A. J. M. Salt-Promoted Catalytic Methanol Carbonylation Using Iridium Pincer-Crown Ether Complexes. *Catal. Sci. Technol.* **2018**, *8*, 3133−3143.
(32) Cammarota, R. C.; Lu, C. C. Tuning Nickel with Lewis Acidic Group 13 Metalloligands for Catalytic Olefin Hydrogenation. *J. Am. Chem. Soc.* **2015**, *137*, 12486−12489.
(33) Forrest, S. J. K.; Clifton, J.; Fey, N.; Pringle, P. G.; Sparkes, H. A.; Wass, D. F. Cooperative Lewis Pairs Based on Late Transition Metals: Activation of Small Molecules by Platinum(0) and $B(C_6F_5)_3$. *Angew. Chem., Int. Ed.* **2015**, *54*, 2223−2227.
(34) Bae, S. H.; Lee, Y.-M.; Fukuzumi, S.; Nam, W. Fine Control of the Redox Reactivity of a Nonheme Iron(III)−Peroxo Complex by Binding Redox-Inactive Metal Ions. *Angew. Chem., Int. Ed.* **2017**, *56*, 801−805.
(35) Park, Y. J.; Cook, S. A.; Sickerman, N. S.; Sano, Y.; Ziller, J. W.; Borovik, A. S. Heterobimetallic Complexes with M^{III}-(μ-OH)-M^{II} Cores (M^{III} = Fe, Mn, Ga; M^{II} = Ca, Sr, and Ba): Structural, Kinetic, and Redox Properties. *Chem. Sci.* **2013**, *4*, 717−726.
(36) Chantarojsiri, T.; Ziller, J. W.; Yang, J. Y. Incorporation of Redox-Inactive Cations Promotes Iron Catalyzed Aerobic C−H Oxidation at Mild Potentials. *Chem. Sci.* **2018**, *9*, 2567−2574.
(37) Younkin, T. R.; Connor, E. F.; Henderson, J. I.; Friedrich, S. K.; Grubbs, R. H.; Bansleben, D. A. Neutral Single-Component Nickel(II) Polyolefin Catalysts That Tolerate Heteroatoms. *Science* **2000**, *287*, 460−462.
(38) Cai, Z.; Xiao, D.; Do, L. H. Fine-Tuning Nickel Phenoxyimine Olefin Polymerization Catalysts: Performance Boosting by Alkali Cations. *J. Am. Chem. Soc.* **2015**, *137*, 15501−15510.
(39) Cai, Z.; Do, L. H. Customizing Polyolefin Morphology by Selective Pairing of Alkali Ions with Nickel Phenoxyimine-Polyethylene Glycol Catalysts. *Organometallics* **2017**, *36*, 4691−4698.
(40) Zhang, D.; Chen, C. Influence of Polyethylene Glycol Unit on Palladium- and Nickel-Catalyzed Ethylene Polymerization and Copolymerization. *Angew. Chem., Int. Ed.* **2017**, *56*, 14672−14676.
(41) Smith, A. J.; Kalkman, E. D.; Gilbert, Z. W.; Tonks, I. A. $ZnCl_2$ Capture Promotes Ethylene Polymerization by a Salicylaldiminato Ni Complex Bearing a Pendent 2,2′-Bipyridine Group. *Organometallics* **2016**, *35*, 2429−2432.
(42) Garden, J. A.; Saini, P. K.; Williams, C. K. Greater than the Sum of Its Parts: A Heterodinuclear Polymerization Catalyst. *J. Am. Chem. Soc.* **2015**, *137*, 15078−15081.
(43) Garden, J. A.; White, A. J. P.; Williams, C. K. Heterodinuclear Titanium/Zinc Catalysis: Synthesis, Characterization and Activity for CO_2/Epoxide Copolymerization and Cyclic Ester Polymerization. *Dalton Trans.* **2017**, *46*, 2532−2541.
(44) Delferro, M.; Marks, T. J. Multinuclear Olefin Polymerization Catalysts. *Chem. Rev.* **2011**, *111*, 2450−2485.
(45) Wei, J.; Shen, Z.; Filatov, A. S.; Liu, Q.; Jordan, R. F. Self-Assembled Cage Structures and Ethylene Polymerization Behavior of Palladium Alkyl Complexes That Contain Phosphine-Bis(arenesulfonate) Ligands. *Organometallics* **2016**, *35*, 3557−3568.
(46) Johnson, L.; Wang, L.; McLain, S.; Bennett, A.; Dobbs, K.; Hauptman, E.; Ionkin, A.; Ittel, S.; Kunitsky, K.; Marshall, W.; McCord, E.; Radzewich, C.; Rinehart, A.; Sweetman, K. J.; Wang, Y.; Yin, Z.; Brookhart, M. Copolymerization of Ethylene and Acrylates by

DOI: 10.1021/acs.organomet.8b00561
Organometallics XXXX, XXX, XXX−XXX

Nickel Catalysts. In *Beyond Metallocenes*; American Chemical Society: Washington, DC, 2003; Vol. *857*, pp 131−142.
(47) Renny, J. S.; Tomasevich, L. L.; Tallmadge, E. H.; Collum, D. B. Method of Continuous Variations: Applications of Job Plots to the Study of Molecular Associations in Organometallic Chemistry. *Angew. Chem., Int. Ed.* **2013**, *52*, 11998−12013.
(48) Smith, J. B.; Kerr, S. H.; White, P. S.; Miller, A. J. M. Thermodynamic Studies of Cation−Macrocycle Interactions in Nickel Pincer−Crown Ether Complexes Enable Switchable Ligation. *Organometallics* **2017**, *36*, 3094−3103.
(49) Saeed, M. A.; Fronczek, F. R.; Hossain, M. A. Encapsulated Chloride Coordinating with Two In-In Protons of Bridgehead Amines in an Octaprotonated Azacryptand. *Chem. Commun.* **2009**, 6409−6411.
(50) Dudkina, Y. B.; Kholin, K. V.; Gryaznova, T. V.; Islamov, D. R.; Kataeva, O. N.; Rizvanov, I. K.; Levitskaya, A. I.; Fominykh, O. D.; Balakina, M. Y.; Sinyashin, O. G.; Budnikova, Y. H. Redox Trends in Cyclometalated Palladium(II) Complexes. *Dalton Trans.* **2017**, *46*, 165−177.
(51) Therrien, J. A.; Wolf, M. O.; Patrick, B. O. Electrocatalytic Reduction of CO_2 with Palladium Bis-*N*-heterocyclic Carbene Pincer Complexes. *Inorg. Chem.* **2014**, *53*, 12962−12972.
(52) Brown, I. D.; Skowron, A. Electronegativity and Lewis Acid Strength. *J. Am. Chem. Soc.* **1990**, *112*, 3401−3403.
(53) Delgado, M.; Ziegler, J. M.; Seda, T.; Zakharov, L. N.; Gilbertson, J. D. Pyridinediimine Iron Complexes with Pendant Redox-Inactive Metals Located in the Secondary Coordination Sphere. *Inorg. Chem.* **2016**, *55*, 555−557.
(54) Ma, Z.; Yang, W.; Sun, W.-H. Recent Progress on Transition Metal (Fe, Co, Ni, Ti and V) Complex Catalysts in Olefin Polymerization with High Thermal Stability. *Chin. J. Chem.* **2017**, *35*, 531−540.
(55) Rhinehart, J. L.; Brown, L. A.; Long, B. K. A Robust Ni(II) α-Diimine Catalyst for High Temperature Ethylene Polymerization. *J. Am. Chem. Soc.* **2013**, *135*, 16316−16319.
(56) Rhinehart, J. L.; Mitchell, N. E.; Long, B. K. Enhancing α-Diimine Catalysts for High-Temperature Ethylene Polymerization. *ACS Catal.* **2014**, *4*, 2501−2504.
(57) Ikeda, S.; Ohhata, F.; Miyoshi, M.; Tanaka, R.; Minami, T.; Ozawa, F.; Yoshifuji, M. Synthesis and Reactions of Palladium and Platinum Complexes Bearing Diphosphinidenecyclobutene Ligands: A Thermally Stable Catalyst for Ethylene Polymerization. *Angew. Chem., Int. Ed.* **2000**, *39*, 4512−4513.
(58) Kim, T.-J.; Kim, S.-K.; Kim, B.-J.; Hahn, J. S.; Ok, M.-A.; Song, J. H.; Shin, D.-H.; Ko, J.; Cheong, M.; Kim, J.; Won, H.; Mitoraj, M.; Srebro, M.; Michalak, A.; Kang, S. O. Half-Metallocene Titanium(IV) Phenyl Phenoxide for High Temperature Olefin Polymerization: Ortho-Substituent Effect at Ancillary *o*-Phenoxy Ligand for Enhanced Catalytic Performance. *Macromolecules* **2009**, *42*, 6932−6943.
(59) Dai, S.; Sui, X.; Chen, C. Highly Robust Palladium(II) α-Diimine Catalysts for Slow-Chain-Walking Polymerization of Ethylene and Copolymerization with Methyl Acrylate. *Angew. Chem., Int. Ed.* **2015**, *54*, 9948−9953.
(60) Woo, T. K.; Ziegler, T. The Influence of Electronic and Steric Factors on Chain Branching in Ethylene Polymerization by Brookhart-type Ni(II) Diimine Catalysts: A Combined Density Functional Theory and Molecular Mechanics Study. *J. Organomet. Chem.* **1999**, *591*, 204−213.
(61) Zhang, W.; Waddell, P. M.; Tiedemann, M. A.; Padilla, C. E.; Mei, J.; Chen, L.; Carrow, B. P. Electron-Rich Metal Cations Enable Synthesis of High Molecular Weight, Linear Functional Polyethylenes. *J. Am. Chem. Soc.* **2018**, *140*, 8841−8850.
(62) Zhang, F.; Wang, L.; Chang, S.-H.; Huang, K.-L.; Chi, Y.; Hung, W.-Y.; Chen, C.-M.; Lee, G.-H.; Chou, P.-T. Phosphorescent Ir(III) Complexes with Both Cyclometalate Chromophores and Phosphine-Silanolate Ancillary: Concurrent Conversion of Organosilane to Silanolate. *Dalton Trans.* **2013**, *42*, 7111−7119.
(63) Rülke, R. E.; Ernsting, J. M.; Spek, A. L.; Elsevier, C. J.; van Leeuwen, P. W. N. M.; Vrieze, K. NMR Study on the Coordination Behavior of Dissymmetric Terdentate Trinitrogen Ligands on Methylpalladium(II) Compounds. *Inorg. Chem.* **1993**, *32*, 5769−5778.
(64) Daugulis, O.; Brookhart, M.; White, P. S. Phosphinidine-Palladium Complexes for the Polymerization and Oligomerization of Ethylene. *Organometallics* **2002**, *21*, 5935−5943.

DOI: 10.1021/acs.organomet.8b00561
Organometallics XXXX, XXX, XXX−XXX